2013

Quantitative Evidence of Reaction During Hypervelocity Penetration of Aluminum Through Oxygenated Fluids

Moore, Joseph

Available online at www.sciencedirect.com

SciVerse ScienceDirect

Procedia Engineering 58 (2013) 157 – 166

Procedia Engineering

www.elsevier.com/locate/procedia

The 12th Hypervelocity Impact Symposium

Quantitative Evidence of Reaction During Hypervelocity Penetration of Aluminum Through Oxygenated Fluids

Joseph Moore[a], Christoph Gloßner[b], William Craig[a], Marek Dolak[a]

Max Peters[a], Manfred Salk[b], Nick Glumac[c], Ronald E. Brown[a] *

[a]*United States Naval Postgraduate School, Monterey, CA 93943*
[b]*Ernst Mach Institut, Freiburg, Germany*
[c]*University of Illinois, Urbana-Champagne, Illinois*

Abstract

Qualitative evidence of chemical reactions between combustible metal shaped charges in air and water has previously been reported based on high-speed photography, spectroscopy, and calorimetry. This report covers investigations directed towards quantifying the conditions under which reaction occurs and the consequences on terminal encounter with submerged inert steel plates. In order to distinguish effects hypervelocity long-rod and shaped charge jet impact experiments were conducted in inert fluid, water and concentrated hydrogen peroxide. It is shown that reaction causes foreshortening of aluminum penetrators at rates that are more competitive at impact velocities towards the slow end of an effective penetrating jet, and that localized reaction and thermal expansion of ablative particulates prior to and after impact can cause substantial plate deformation. The results are consistent with hydrodynamic penetration theory when modified for reaction induced foreshortening. Predicted impact and penetration effects against submerged steel plates submerged in a chemically inert fluid are shown to agree with experiment, and the effect of density difference between the selected spindle oil inert simulant, water and concentrated hydrogen peroxide are shown to be within experimental variation.

Selection and peer-review under responsibility of the Hypervelocity Impact Society

1. Introduction

The oxidative potential of aluminum is well known and very much studied. Aluminum is commonly added to propellants to increase specific impulse and to explosives to increase blast and overpressure. In those applications, oxidizers are in the gas-phase, but reaction of aluminum in liquid water media is also energetic and widely studied. Molten aluminum dropped into water has been observed to spontaneously explode with yields comparable to equivalent amounts high explosive. Such "steam explosions" have been investigated in depth, primarily for foundry or reactor safety reasons [1]. In ballistic applications, its chemical potential is exploited for increasing air and water blast under conditions when the metal can be rapidly particulated either by impact or by explosive dispersal. On the other hand it is rarely if ever considered as a factor during hypervelocity impact and penetration. Rather the primary interest has focused on understanding more thoroughly density and compression effects. With respect to shaped charge performance aluminum is usually considered as a liner material for those cases where faster coherent jetting and larger target perforating capability are desired compared to those from more traditional copper-lined charges (i.e., all other things equal). However, Glumac and co-workers reported qualitative evidence of aluminum reaction with water during hypervelocity penetration based on high-speed photography,

* Corresponding author. Tel.: +1-831-656-2635; fax: +1- 831-656-2834.
E-mail address: rebrown@nps.edu.

Selection and peer-review under responsibility of the Hypervelocity Impact Society
doi:10.1016/j.proeng.2013.05.019

spectroscopy, calorimetry, and post-test chemical analyses of collected residues [2]. We report herein additional and more direct evidence of chemical effects during the hypervelocity impact and penetration of aluminum long-rods and jets, under conditions most favorable for oxidation reaction (i.e., impacts against plates submerged in an oxidizing fluid), which can lead to penetration decrease.

Reaction of aluminum with water proceeds as follows;

$$Al + 3H_2O \rightarrow Al(OH)_3 + \frac{3}{2}H_2 + 15.4 \text{ kjoules/gram} \quad (1)$$

Hydrogen can react with the oxygen in water to release an additional 10.6 kjoules/gram, however, this additional energy is ignored.

2. The Paradox

While previous reported investigations of aluminum jet penetration through water by Cullis and Sinden [3] and Held and Backofen [4] lack any identification of chemical effects, it is important to understand that compressional effects could very well have been concluded as the exclusive cause of penetration decrements relative to Bernoulli hydrodynamic theory [5,6]. Compression between the bow shock and jet tip can cause jet foreshortening and penetration potential decrease [7]. Pre-impact chemical-induced erosion of a combustible penetrator against submerged plates could lead to similar penetration trend for cases where engagement with water is relatively substantial. On the other hand, one might expect reactivity to increase plate damage particularly from the collective and concentrated particulation during impact and penetration. Yet, any chemical-induced foreshortening prior to impact and penetration can mask results from the overall mechanism.

We show in this report clear evidence of the erosive effect on inert plate penetration and on plate deformation, by direct comparisons between impacts against steel plates submerged in an inert fluid close in density to water, water and concentrated hydrogen peroxide. In the latter case, the necessity of taking into account chemically induced foreshortening in the overall analyses of deformation and penetration is critical since it is clear that rod and jet lengths are affected by travel distance through reactive fluids prior to plate impact.

3. Outline of Investigation

Additional qualitative evidences of reaction are observed photographically. In this case, reaction is evident at lower velocities than those previously reported along the bow of combustible shaped charge jets. The cumulative effects of chemical energy during impact and penetration of a long *l/d* aluminum rod is shown, attesting to the possibilities of prompt free surface exposure resulting from rapid near-impact erosion, and particulation during impact and friction during penetration. The overall effect of faster impacts from aluminum shaped charge jet pulls together the lesson learned from the controlled rod penetration investigations.

4. Experimental Approach

Both controlled long rod aluminum penetration tests, as well as aluminum-lined shaped charge tests were performed against steel plates submerged in an inert oil, water and concentrated hydrogen peroxide (30%). Tests conducted against plates submerged in oil provide bases for assessing the effects of oxidation, while tests in peroxide represent perhaps a reaction limit.

4.1. Controlled Gas-Gun Launched Tests

Long rod aluminum projectiles were controlled launched from an EMI Free-Flight Light (2-stage) Gas Gun into an attached two-compartment ballistic chamber see Fig 1. The rods were encapsulated in a composite pusher/sabot composed, respectively of polycarbonate/aluminum. Both sabot and pusher were separated from the penetrator after discharge midway in an atmospherically controlled ballistic tank connected to the gun. Interruption of a pair of laser beams, at calibrated distance separation was used to estimate rod velocity and to trigger downstream stationed flash x-rays; including a pair for recording sabot separation; and another pair of x-rays for recording rod orientation and velocity just prior to entrance into an expandable target chamber. High-speed video cameras were also employed for recording projectile flight from target chamber approach to impact.

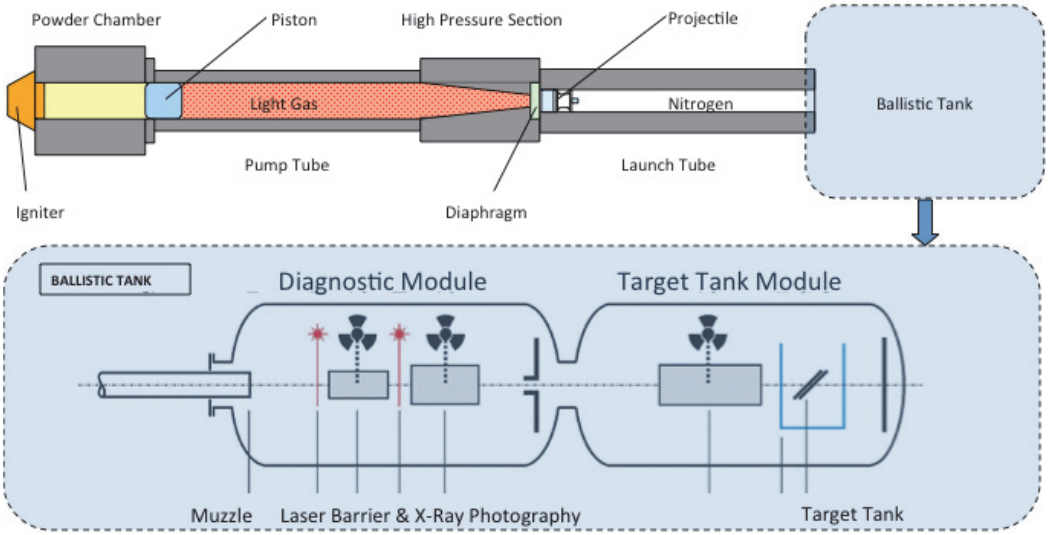

Fig. 1. Schematic of the EMI Facilities for Investigating the Effects of Chemical Reaction of Combustible Projectiles during Impact and Penetration against Submerged Steel Plates: Projectile entry and typical target arrangement in the @46-degree obliquity in the target tank is shown in Figure 2.

Propellant charges were designed to launch rods at velocities between 2.7 and 3.5 km/sec. Most of the tests were conducted between 2.7 to 2.9 km/sec.

Expendable Plexiglas chambers were used to house fluid and steel target plates in the second compartment of the ballistic chamber. The plates were mounted at 45 degrees, as shown in Fig 2. A polyethylene film thin enough to prevent fluid leakage prior to projectile impact covered the "diaphragm aperture". The Plexiglas tanks themselves were installed in a steel tub on the floor of the ballistic chamber.

Plates were constructed of steel with overall width and length dimensions of 200 by 280mm. Three type of plates were used: A single plate at 20mm thickness; a spaced configuration consisting of two 10mm thick plates separated by 10mm; and a third configuration consisting of a 5mm frontal plate backed by a 15mm plate at 10mm separation.

4.2. Shaped Charge Tests

Precision 50mm aluminum lined shaped charge were fabricated for tests conducted to determine penetration at faster impact velocities. They were point initiated and fired at a constant standoff of 190mm from the entry to a submerged spaced plates array as shown in Fig 3. The array consisted of 3.3mm thick mild steel plates spaced 22.9mm from each other.

4.3. Materials

The rods used for the rod impacts consisted of aluminum 1100-0, machined to final dimensions of 6.5mm diameter by 130mm length. Aluminum 6061 was used for the shaped charge liners. Water and 30 percent hydrogen peroxide [6] were used to study projectile-fluid and jet-fluid reactions. Shell Morlina 10 "spindle" oil [7] was used as a close-to-water density inert fluid.

5. Finite Difference Simulations

The ANSYS AUTODYN explicit dynamics code and the Sandia National Laboratory CTH Eulerian processor were employed for simulating impact and penetration behavior. Both codes have been validated under wide ranges of conditions dealing with explosive detonation, shaped charge jetting, and impact and penetration. AUTODYN was mostly employed. In all cases zoning resolution was studied for each series of simulations to insure optimal zoning. Transmit and flow-out boundaries along with mesh size were set to minimize shock reflection effects and to estimate jet velocity-mass distribution characteristics, respectively. Parameters for the Johnson-Cook material response model [8] built into the code library were used. Penetration data reported by Anderson et al. [9,10] were used to validate computational techniques over specific impact velocity ranges close to those studied.

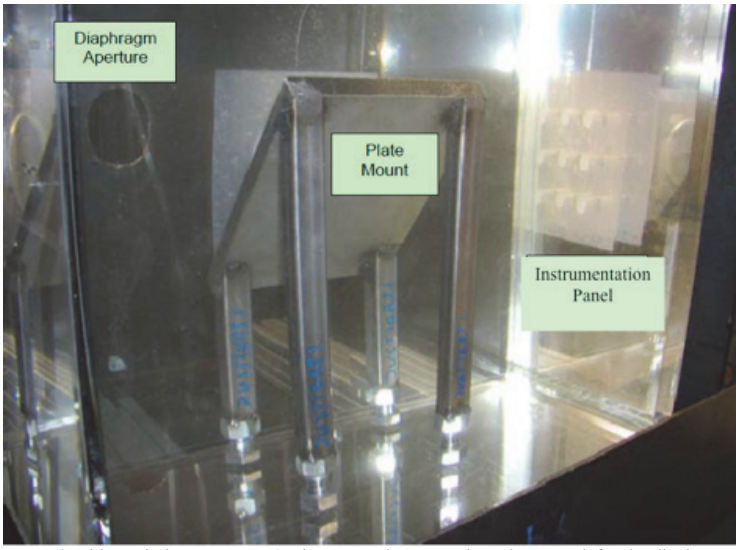

Fig. 2. Expendable Plexiglas target tank with steel plate mount at 45-degree. Rod entrance is at the upper left. The diaphragm aperture was covered with a thin polyethylene film. The target tank is housed in a steel tub that catches fluid escape and debris.

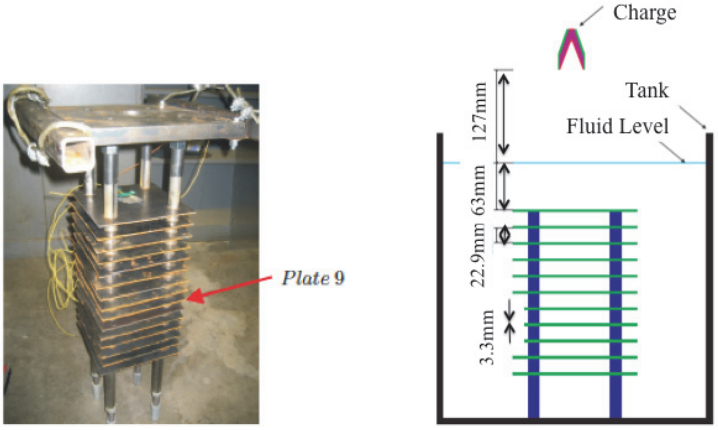

Fig. 3. Test setup for shaped charge jet impact tests. Plate 9 is a significant position since this is near penetration termination.

6. Experimental Conditions and Results

Whereas, possible evidences of combustible metal-water reactions were found about the tip regions in shaped charge jets, these studies initially focused at impact velocities that would be more characteristic of the tail regions of a jet (i.e., 2-3 km/sec). It was presumed that because of the general manner in which a shaped charge liner partitions mass, potential chemistry should increase along the jet length where velocities are much slower than at the tip but still faster than effective ballistic limits. Experimental control of conditions at this velocity range is also much greater with the accommodation of light gas launch. Results from these initial efforts provided additional validation of computational accuracies as well. For example, the development, location and geometric contour of the high-pressure bow shock recorded forward of aluminum rods penetrating through water were found to closely match prediction, as shown in Fig 4. It is of interest to note that the bow shock in dense liquid media can exert sufficient pressure to soften and deform thin targets [11], which is an important consideration.

6.1. Supporting Qualitative Evidence of Chemical Reaction and Foreshortening

Glumac et al. [2] reported bright illuminations along the tips of aluminum and other combustible metal jets traveling through water. There were no similar indications of reaction along the mid-section and tail of the jets. We show such

behavior at velocities in aluminum rod impact at velocities (i.e., 2.75 km/sec) that would be at the slowest portion of a jet from high frame rate video recordings reported in Fig 5. The videos in the figure are of aluminum rods impacting and penetrating the oil, water and 30% hydrogen peroxide fluids prior to oblique target-plate impact. The distance between rod entrance into the Plexiglas target chamber and plate impact is 12cm. The average velocity through the fluids is 1.49 km/sec.

The entry times into the target chamber vary slightly from test to test. However, it is obvious from the video frames that rod erosion during transit through peroxide is much greater than those through the oil and water media (see last frames for each penetrated fluid). This video coverage is representative of results from 14 tests.

6.2. Effect of Foreshortening and Reaction on Target Deformation and Perforation by Aluminum Rod Impact

Fig 6 shows the damage to the oblique 20mm thick steel plates submerged in oil, water and peroxide resulting from rod impacts at 2.7 km/sec. The impacted plates in each case were almost perforated; as evidenced by severe bulging and cracking on their backsides. Rod penetration of the submerged plates in peroxide was the greatest; followed by the plates submerged in water and oil. Yet, there is evidence from the video coverage that the rod transiting through peroxide before impact might have undergone a greater amount of erosion than the others. Volumetric displacements in the actual plates varied by only 10 percent, with the order of displacement greatest for the target submerged in oil, followed by the one in water. The plate submerged in peroxide was deformed the greatest. Alumina deposits found on the impacted surface of the plates submerged in water and peroxide are evidence of chemical reaction.

The effect of chemical reaction is somewhat less apparent from results against the spaced 10+10 mm plates (see Table 1). The front 10mm plate in all cases was penetrated and the residual rods came to rest in the second plates. Hole volumes displaced in the aft plates, varied between 3000 and 4000 mm^3 irrespective of the submerging fluid. In fact the largest volume displaced against plates submerged in peroxide was approximately the same as those displaced in plates submerged in oil. Plate deformation of targets in the peroxide was also slightly greater.

A substantial blast effect resulted from the impact against the 5+15 mm steel plate submerged in peroxide. A comparison between the damage caused in this case and that resulting from a like impact against plates submerged in water is shown in Fig 6. Alumina deposits surround the holes in each of these plates. Damage against these targets submerged in oil was close to that shown for the water-submerged target.

Computational predictions were found to compare favorably with results for rod impacts against the oil-submerged targets (i.e., taking into account projectile strength, rod orientation at impact, and line-of-sight transit through the fluid). On the other hand penetration against the targets submerged in water and peroxide were over-predicted. Computational estimates of the hydrodynamic projectile also indirectly support the possibilities of chemical erosion. That is, residual penetrator lengths and kinetic energies at plate impact were greater than actual; with the differences greater for the tests conducted in hydrogen peroxide than those in water.

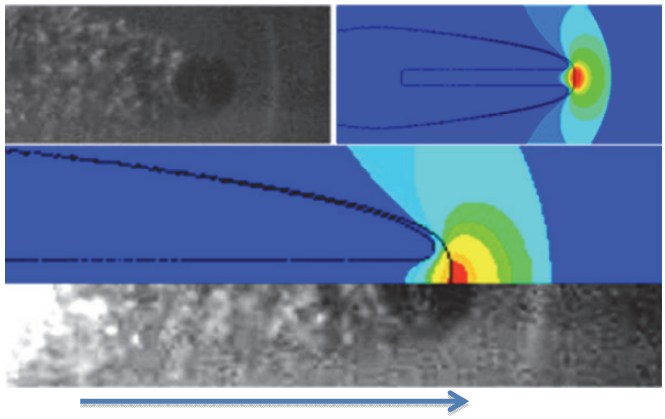

Fig. 4. Observed (upper-left) and predicted (upper right) bow shock resulting from an impact in water of the 6.5mm diameter l/d 20 rod at 3.25 km/sec and comparison at identical time after impact.

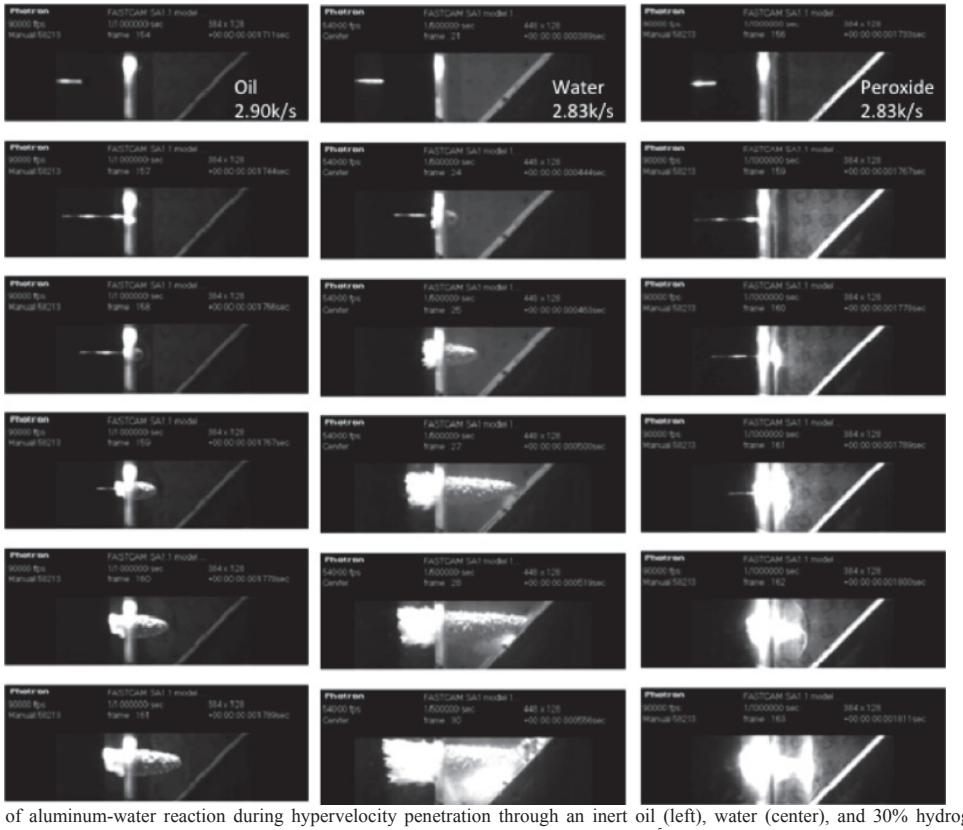

Fig. 5. Evidence of aluminum-water reaction during hypervelocity penetration through an inert oil (left), water (center), and 30% hydrogen peroxide (right), after impacting the fluids at the respective velocities. High-speed video framing rate is at $9 \cdot 10^5$ frames/sec. Resultant plate deformation and holing are shown in Fig 6.

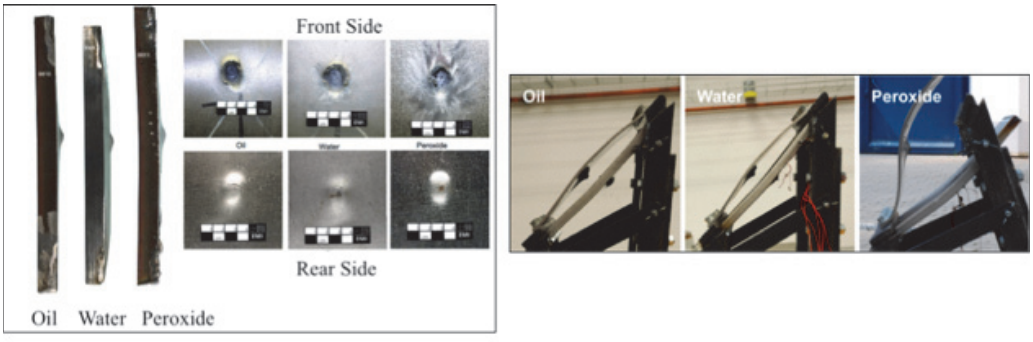

(left) (right)

Fig. 6. (left) Plate deformation and holes in submerged 20mm steel plates resulting from aluminum rod impacts: (right) Effect of Submerging Fluid on Deformation of the 5+15mm Plate Array.

Table 1 Damage from Aluminum Projectile Impacts Against Submerged 20mm Thick Steel Plates

Fluid	Impact Velocity	Bend Angle	Hole Length	Hole Width	Cavity Cross Section	Cavity Volume	Cavity Depth
	(km/sec)	(degrees)	(mm)	(mm)	(mm^2)	(mm^3)	(mm)
Oil	2.90	3.1	20.0	14.1	331	4100	19.4
Water	2.83	2.8	21.6	13.5	312	3700	19.1
Peroxide	2.84	5.6	22.4	13.6	301	3000	17.6

6.3. Effect of Reaction on Shaped Charge Jet Penetration

The cumulative effects of reaction during the transit, impact and penetration are shown in a series of test-conducted firings of 50mm aluminum-lined shaped charge against spaced steel plate arrays (see Fig 3) submerged in oil and water.

A total of six shaped charge tests were conducted using the experimental setup described in Fig 3. One of the tests was conducted against targets submerged in oil and the remaining ones conducted against those submerged in water. The standoff distance between the charge base and first target plate is 190 mm. In two water tests, the jet reached plate 8. In the other tests the jet reached either plate 9 or 10. In all cases, significant deformation was observed in the last plate penetrated, as well as the plate below it. Peak displacements of approximately 11 mm were observed, and the visible deformation extended out to the edge of the 20 cm square plates. For the test conducted in oil, no significant plate deformation was observed, though the jet reached plate 9. There were no statistically significant differences in hole diameters for all six tests. Time-of-arrivals between the jet impacted in the oil submerged target did differ with the averages impacted transiting through the water-submerged target. Additional tests against submerged targets containing plates of different thicknesses further confirmed our interpretation of experimental penetration rates and computational predictions. Average jet tip velocity, measured using two laser light trip beams to detect jet tip motion, is 6.3±0.1 km/s. The predicted velocity from AUTODYN computation is 6.2 km/s. Estimated effective jet mass is 4.4 grams, which is 20 per cent of the liner mass. The only major difference was the observation of enhanced deformation in the final target plates (Fig 7).

Prior to the tests, computations were performed to determine the degree of difference in penetration resistance to (i) a 10mm diameter by 50mm long copper rod at 5 km/s impact velocity and (ii) the jet from the 50mm aluminum lined shaped charge. Differences between square-root hydrodynamic penetration theory, including penetrator strength, and AUTODYN simulation with built-in shock equation of state models were found to be 4.2 and 3.2 percent, respectively, for the copper rod problem. The mean difference between predicted shaped charge jet penetrations through the submerged target array varies by 1.9 per cent.

This is the difference in time of arrival between water and oil at each target plate (see Fig 7).

The difference in jet time of arrival along the penetration path, as monitored at each plate, gradually increases at an increasing rate from 2 to 8.6 per cent, which is a reflection of the basic difference in fluid densities, increase in potential reactive aluminum mass along the tail regions of the jet, and competitive rates between reaction and penetration.

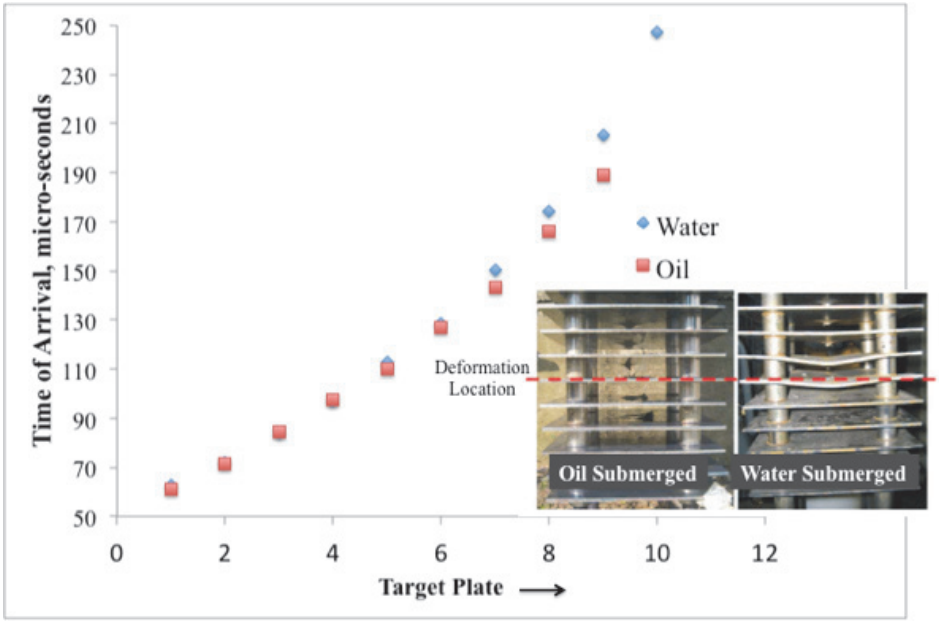

Fig. 7. Effect of chemical-induced foreshortening of the aluminum jet and more massive reaction along the jet tail causing plate deformation.

7. Discussion of Results

With respect to the single aluminum rod impacts, average aluminum impact velocities against the fluids is between 2.74 and 2.76 km/sec, and the standard deviations vary from 0.05 to 0.09 km/sec. Velocities through the fluids do not follow strength-less hydrodynamic theory, which in these cases would be 1.71-1.72 km/sec. Actual average velocities, *u,* through the fluids are between 1.45 and 1.53 km/sec with similar deviation range. The differences are accounted for based on Johnson-Cook parameters and are consistent with the modified Bernoulli equation and close to reported dynamic yield value of aluminum reported by Allen and Rogers [12], see Eq. (3) where there is shown the functional relationship between penetration velocity *u* and impact velocity (*v)*, penetrator and fluid velocities density (resp. ρ_p and ρ_f), and penetrator strength (ϕ_p).

$$u = \frac{\rho_o v - \left[\rho_p v^2 - 2(\rho_p - \rho_f)\left(\frac{1}{2}\rho_p v^2 - \Phi_p\right)\right]^{1/2}}{\rho_p - \rho_f} \tag{2}$$

Evidence presented supports chemical contributions to foreshortening of combustible projectiles in water and the potential of rapid particulate reaction at impact after impact, particularly against spaced plate arrays that can cause plate deformation. Pre-impact conditioning (i.e., bow shock effect) leading to target weakening and deformation itself cannot be discounted, however, based on the results reported. However, it is readily apparent that chemistry contributes to the expansive dismemberment of spaced plates.

Understanding the effects to direct penetration is accomplished taking into account pre-impact erosion. As previously mentioned significant effort was expended in order to validate the material models and computational techniques and post-processors previously developed with the AUTODYN explicit dynamics code. Additional confidences in predictability included the bow wave simulation (see Fig. 4) and 3D impact/penetration simulations, an example of which is shown in Fig 8.

The use of an inert oil and concentrated hydrogen peroxide provide means for identifying not only the effects of oxidative reaction but also allows one to distinguish effects in water that might have been dismissed because of experimental uncertainty. The effect of reaction against the monolithic 20mm and the spaced 5+15mm target can be clearly associated with aluminum reaction; however, actual hole displacement is a real indication of physical and chemical contributions to penetration since the rods erode somewhat prior to impact. In order to determine these contributions the following were performed:

- Penetrator length at impact and hole volumes were predicted based on actual impact conditions, incl., velocity, pitch and yaw.
- The true dynamic strength of the target plate is estimated based on the kinetic energy dissipated during penetrator impact and the resulting hole in the oil submerged target.
- Chemical energy contributions are estimated (see Table 2) based on differences between experimental hole volume and those estimated based on kinetic energy dissipation alone.

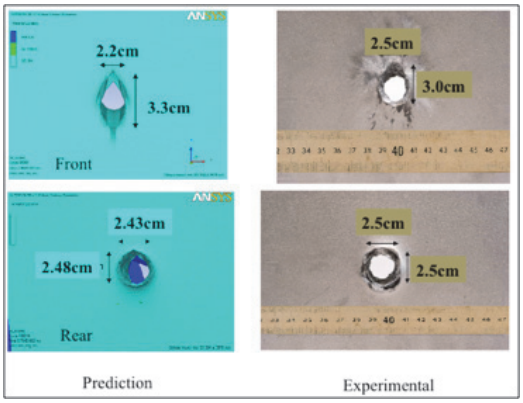

Fig. 8. Comparison of experimentally observed and predicted hole in a water-submerged steel plate resulting from the impact of a long rod aluminum projectile at 3.6 km/sec. The slight difference between simulation and prediction is attributed to chemical interactions.

Compounded predictions of shaped charge jetting and penetration appear to revalidate developed computational approaches using AUTODYN, based on the extremely good fits with time-of-arrival data for the oil-submerged case. Small amounts of off-axis drift along the tail regions of the jet and hole narrowing result in less total penetration than predicted.

This is also not surprising since jet velocity drops off below 1 km/sec past the tenth plate. Small deformations in the first three or four plates result from the slug. Estimated total effective length of jet, l_{jet} is 293 mm by Eq. 3, where n is the number of plates penetrated (i.e., n = 9) and the standoff distance, s, is 190mm. This length is confirmed in another test against water submerged 101.6 mm thick steel at the same standoff distance in which the jet stopped just before breakthrough.

$$l_{jet} = (n+1)t_{steel}\left(\rho_{steel}/\rho_{aluminum}\right)^{1/2} + (s+nt)\left(\rho_{water}/\rho_{aluminum}\right)^{1/2} \tag{3}$$

Glumac reports temperature conditions for aluminum reaction in the neighborhood of 1700-1800^{o}. It is therefore of interest to estimate whether these conditions are consistent with the computational schemes employed. We addressed this problem using zoom-in features in AUTODYN and continual refinement of the steady-state internal energy contour along the aluminum-water impact and erosion front. Cell by cell changes in internal energy in the aluminum and water are then used in a post-processor to convert internal energy to temperature taking into account specific heats, state-transition enthalpies and the thermodynamic effects of pressure and volume change. Estimated mixed melt starts of aluminum and water vapor along portions within the erosion front that are much below aforementioned reaction conditions. However, we have not included the effects of pre-target impact compression and resultant post impact aluminum particulation, which will probably exceed reaction threshold for "cold" rod and "hot" jet impact.

It is important to note that the slug from the shaped charge comes to rest and/or lodges no further than Plate 4 and that the there was only negligible deformation in the plates submerged in the oil fluid.

8. Conclusions

Clear evidence of aluminum projectile reaction during hypervelocity impact and penetration through water and impact against steel targets are shown at impact velocities between 2.7 and 6 km/sec. Reaction accelerates erosive foreshortening of the projectile, however, under conditions where the transit distance to the target is relatively short, damage can more than compensate for the projectile length decrease with respect to target displacement and deformation. Computational techniques are shown to accurately predict non-chemical aspects of the process as exemplified by observed comparisons with impact experiments conducted against steel plates submerged in an inert fluid, and the importance of taking into account the effect dynamic strength on hydrodynamic penetration is reinforced. It is also shown that accurate prediction of the physical and kinetic processes provides confident estimate of chemical contributions to plate deformation by difference.

The time of arrival data and predicted jet mass from the shaped charge results provide a means for estimating energy deposition between plates, reported in Fig 9. The simulation result is based on the jet mass that would be deposited between plates from a perfectively straight jet. The other plot in Figure 9 is based on matching the time of arrivals and corresponding jet velocities and jet masses predicted in the simulation. The potential energies are a product of mass and thermochemical energy leading to aluminum hydroxide. Based on these results, the energy available for causing target deformation in plates 8, 9 and 10 is between 14 and 22 kilojoules.

Table 2. Estimated Chemical Energy Contribution, in kjoules, to Target Displacement Resulting from Aluminum Rod (l/d=20) Impact at Between 2.7 and 2.8 km/sec in Per cent of Total Hole Volume Measured.

Fluid/Target	20mm	10+10mm 1st Plate	10+10mm 2nd Plate	5+15mm 1st Plate	5+15mm 2nd Plate
Oil	0	0	0	0	0
Water	3.1	3.6	4.3	(small)	3.3
Peroxide	8.8	6.0	16.1	(small)	32.7

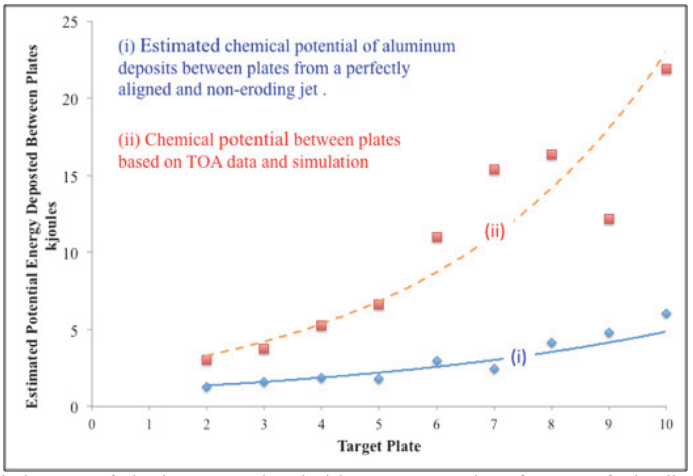

Fig. 9. Estimated potential chemical energy of aluminum mass deposited between target plates from a perfectly aligned jet and from the averaged experimental jets.

References

[1] Nelson, L.S., 1995, “Steam explosions of single drops of pure and alloyed molten aluminum, ”Nuclear Engineering and Design, v.55, pp. 413-425.
[2] Glumac, N., et al., 2007. “Effect of Hydroreaction on the Hypervelocity Penetration”, 23rd International Symposium on Ballistics, Tarragona, Spain, v. II, p. 1519.
[3] Cullis, I.G., Sinden, A.W., 1981. “Hypervelocity Projectile Penetration in Water”, 6th International Symposium on Ballistics, Orlando, FL, p. 273.
[4] Held, M., Backofen. J.E., 1990. “Penetration of Shaped Charge Into Water”, 12th International Symposium on Ballistics, San Antonio, TX, v. II, p. 30.
[5] Tate, A., 1967. “A Theory For The Deceleration Of Long Rods After Impact”. Journal of the Mechanics and Physics of Solids, v. 15, p. 387.
[6] Hohler, V., Stilp., 1987. A.J. “Hypervelocity Impact of Rod Projectiles with L/D 1 to 32”, International Journal Impact Engineering, v. 5, p. 323.
[7] Chick, M., Bussell, and Linnane, A.P., 1992.“Water Penetration by High Velocity Projectiles”, 11th Australian Fluid Mechanics Conference, University of Tasmania, Australia, p. 3E-4
[8] Shell Morlina Oil 10,(http://www.epc.shell.com/Docs/GPCDOC_X_cbe_24855_key_140002230957_1634.pdf).
[9] Johnson, G.R., Cook, W.H., 1983. "A Constitutive Model And Data For Metals Subjected To Large Strains, High Strain Rates And High Stress", International Symposium on Ballistics, p. 541.
[10] Anderson, C.E., Wilbeck, J.S., Elder, J.S., 1999. “Long Rod Penetration into Highly Oblique Water-Filled Targets”, International Journal Impact Engineering, v. 23, p. 1.
[11] Anderson, C.E., Morris, B.L., Littlefield, D.L., 1992. “A Penetration Mechanics Database”, Southwest Research Institute Report 3593/001.
[12] Hains, F.D., 1982. “Target Loading from an Underwater Shaped Charge”. Naval Surface Weapons Center, Technical Report 82-168.
[13] Allen W.A., Rogers, J.W., 1961. “Penetration of a Rod into a Semi-Infinite Target”, Journal of the Franklin Institute, v. 272, p. 272.